Publicación Electrónica
ASOCIACIÓN PALEONTOLÓGICA ARGENTINA

www.peapaleontologica.org.ar

Kaijutitan maui, a sauropod titanosaur from the Upper Cretaceous (Sierra Barrosa Formation, Neuquén Basin) of northern Patagonia Argentina: histological and taphonomic considerations

LEONARDO SEBASTIÁN FILIPPI[1]
ELENA PREVITERA[2]
ALBERTO CARLOS GARRIDO[3,4]

1. Museo Municipal "Argentino Urquiza". Chos Malal 1277, 8319 Rincón de los Sauces, Neuquén, Argentina.
2. Instituto Argentino de Nivología, Glaciología y Ciencias Ambientales (IANIGLA CONICET), Universidad Nacional de Cuyo (UNCuyo), Gobierno de Mendoza. Av. Adrián Ruiz Leal s/n, Parque General San Martín CC 330, 5500 Mendoza Capital, Mendoza, Argentina.
3. Museo Provincial de Ciencias Naturales "Profesor Dr. Juan A. Olsacher", Dirección Provincial de Minería. Etcheluz y Ejército Argentino, 8340 Zapala, Neuquén, Argentina.
4. Departamento Geología y Petróleo, Facultad de Ingeniería, Universidad Nacional del Comahue. Buenos Aires 1400, 8300 Neuquén Capital, Neuquén, Argentina.

Recibido: 18 de julio 2023 - **Aceptado:** 26 de febrero 2024 - **Publicado:** 17 de abril 2024

Para citar este artículo: Leonardo Sebastián Filippi, Elena Previtera, & Alberto Carlos Garrido (2024). *Kaijutitan maui*, a sauropod titanosaur from the Upper Cretaceous (Sierra Barrosa Formation, Neuquén Basin) of northern Patagonia Argentina: histological and taphonomic considerations. *Publicación Electrónica de la Asociación Paleontológica Argentina* 24(1): 129–148.

Link a este artículo: http://dx.doi.org/10.5710/PEAPA/26.02.2024.481

ISSN 2469-0228

Asociación Paleontológica Argentina
Maipú 645 1° piso, C1006ACG, Buenos Aires
República Argentina
Tel/Fax (54-11) 4326-7563
Web: www.apaleontologica.org.ar

ARTÍCULO Año 2024 - 24(1): 129–148
Publicación Electrónica
ASOCIACIÓN PALEONTOLÓGICA ARGENTINA

KAIJUTITAN MAUI, A SAUROPOD TITANOSAUR FROM THE UPPER CRETACEOUS (SIERRA BARROSA FORMATION, NEUQUÉN BASIN) OF NORTHERN PATAGONIA ARGENTINA: HISTOLOGICAL AND TAPHONOMIC CONSIDERATIONS

LEONARDO SEBASTIÁN FILIPPI[1], ELENA PREVITERA[2], AND ALBERTO CARLOS GARRIDO[3,4]

[1]Museo Municipal "Argentino Urquiza". Chos Malal 1277, 8319 Rincón de los Sauces, Neuquén, Argentina. *lsfilippi@gmail.com*

[2]Instituto Argentino de Nivología, Glaciología y Ciencias Ambientales (IANIGLA CONICET), Universidad Nacional de Cuyo (UNCuyo), Gobierno de Mendoza. Av. Adrián Ruiz Leal s/n, Parque General San Martín CC 330, 5500 Mendoza Capital, Mendoza, Argentina. *elena.previtera@gmail.com*

[3]Museo Provincial de Ciencias Naturales "Profesor Dr. Juan A. Olsacher", Dirección Provincial de Minería. Etcheluz y Ejército Argentino, 8340 Zapala, Neuquén, Argentina. *albertocarlosgarrido@gmail.com*

[4]Departamento Geología y Petróleo, Facultad de Ingeniería, Universidad Nacional del Comahue. Buenos Aires 1400, 8300 Neuquén Capital, Neuquén, Argentina.

LSF: https://orcid.org/0000-0003-0743-8294; **EP:** https://orcid.org/0000-0002-6689-5877; **ACG:** https://orcid.org/0000-0002-9882-9567

Abstract. *Kaijutitan maui* is a basal titanosaur from the Sierra Barrosa Formation (Coniacian, Upper Cretaceous), Neuquén Basin, Patagonia Argentina. The Neuquén Basin in northwestern Patagonia, Argentina, holds the most important record of Cretaceous dinosaurs from South America. This work constitutes the first case of taphonomic and histological study of a dinosaur from the Rincón de los Sauces area. *Kaijutitan* is represented by cranial and postcranial materials of an adult individual of huge body size, preserved in clay sediments related to a floodplain environment. Bones were found disarticulated but associated, largely respecting their relative anatomical position. Histological and diagenetic features of bones were analyzed in order to interpret the alteration degree of bone microstructure. Biostratinomic processes inferred are subaerial biodegradation, disarticulation, preburial weathering (cracking and flacking), and abrasion. Fossil-diagenetic processes comprise compaction, deformation, permineralization, and fracturing. Permineralization stages included infilling of bone cavities and fractures with sediments, iron oxides, calcite, or an iron oxide-calcite association during the burial history. Some characteristics suggest that the *Kaijutitan* specimen suffered weathering for a certain period of time before final burial and that biological activity in the carcass acted as a dispersal agent for the bones within the paleontological site.

Key words. Taphonomy. Paleohistology. Titanosaur. Coniacian. Neuquén Group. Sierra Barrosa Formation.

Resumen. *KAIJUTITAN MAUI,* UN SAURÓPODO TITANOSAURIO DEL CRETÁCICO SUPERIOR (FORMACIÓN SIERRA BARROSA, CUENCA NEUQUINA) DEL NORTE DE PATAGONIA ARGENTINA: CONSIDERACIONES TAFONÓMICAS Y ANÁLISIS HISTOLÓGICO. *Kaijutitan maui* es un titanosaurio basal de la Formación Sierra Barrosa (Coniaciano, Cretácico Superior), Cuenca Neuquina, Patagonia Argentina. La Cuenca Neuquina en el noroeste de la Patagonia, Argentina, posee el registro más importante de dinosaurios del Cretácico de América del Sur. Este trabajo constituye el primer caso de estudio tafonómico e histológico de un dinosaurio de la zona de Rincón de los Sauces. *Kaijutitan* está representado por materiales craneales y poscraneales de un individuo adulto de gran tamaño corporal que se conservó en sedimentos arcillosos relacionados con un ambiente de llanura aluvial. Los huesos se encontraron desarticulados pero asociados, respetando en gran medida su posición anatómica relativa. Se analizaron las características histológicas y diagenéticas de los huesos para interpretar el grado de alteración de la microestructura ósea. Los procesos bioestratinómicos que se infieren son la biodegradación subaérea, la desarticulación, la meteorización previa al enterramiento (agrietamiento y descamación) y la abrasión. Los procesos fósil-diagenéticos comprenden compactación, deformación, permineralización y fracturación. Las etapas de permineralización incluyeron el relleno de cavidades óseas y fracturas con sedimentos, óxidos de hierro, calcita o una asociación de óxido de hierro y calcita durante la historia del entierro. Algunas características sugieren que el espécimen de *Kaijutitan* sufrió meteorización durante un cierto período de tiempo antes del entierro final, y que la actividad biológica en el cadáver actuó como un agente de dispersión de los huesos dentro del sitio paleontológico.

Palabras clave. Tafonomía. Paleohistología. Titanosauria. Coniaciano. Grupo Neuquén. Formación Sierra Barrosa.

THE TAPHONOMIC study of a paleontological site allows to explain how it was produced and what changes the fossil record has experienced (Fernández López, 1989). The inference of the taphonomic history of an association of vertebrates allows the identification of agents responsible for this accumulation and also provides information about the sedimentology of the deposit (Behrensmeyer, 1991). Taphonomic studies are also necessary to verify the sedimentological, biochronological, and paleobiological inferences proposed from a given fossil (Alcalá, 1994).

Taphonomic research in Mesozoic reptiles is increasing worldwide and contributing to clarifying palaeoenvironmental, paleontological, and biostratigraphic interpretations (*e.g.*, Paik *et al.*, 2001; Britt *et al.*, 2004, 2009; Eberth *et al.*, 2006; Eberth & Currie, 2010; Brown *et al.*, 2013; Casal *et al.*, 2014; Smith *et al.*, 2015; Dai *et al.*, 2015; Canudo *et al.*, 2016; among others).

The remains of Cretaceous dinosaurs are diverse in South America, mainly in the Neuquén Basin, and most species have been found in Upper Cretaceous strata of the Neuquén Group. Unlike the numerous systematic studies published, sedimentological and taphonomic analyses are scarce (*e.g.*, González Riga & Astini, 2007; Casal *et al.*, 2014, 2023; Previtera, 2011, 2017, 2019a, 2019b) and less frequent than research dealing with phylogeny and palaeobiogeography.

Paleohistology has been revealed as a powerful tool to interpret aspects of dinosaur biology (Chinsamy & Dodson, 1995; Chinsamy-Turan, 2005; Padian & Lamm, 2013; Bailleul *et al.*, 2019). Paleobiological information about tetrapods, such as the degree of ontogenetic development, growth rate, sex, and age (Starck & Chinsamy, 2002; Botha & Chinsamy, 2004; Steyer *et al.*, 2004), as well as fossil diagenetic processes, can be reconstructed through the use of thin bone sections (Bailleul *et al.*, 2019; Jurado *et al.*, 2020). In recent years, numerous paleohistological works have been developed that allowed inferring paleobiological aspects of sauropod dinosaurs (*e.g.*, Klein & Sander, 2008; Stein *et al.*, 2010; Mitchell & Sander, 2014; Mitchell *et al.*, 2017). Actually, advances in assessing dinosaur maturity have notably increased (*e.g.*, Griebeler *et al.*, 2013; Mitchell *et al.*, 2017; Perales-Gogenola *et al.*, 2019; Woodward, 2019).

Here, we present and discuss taphonomic and histological data from the titanosaur sauropod *Kaijutitan maui* Filippi *et al.* (2019), found in the Cañadón Mistringa area (Neuquén, Argentina), integrating different stages of taphonomic preservation with qualitative descriptions of bone microstructure to reconstruct the burial environment. Furthermore, we suggest the ontogenetic stage at the time of the death of the individual, as well as the diagenetic processes suffered by the bones during fossilization.

GEOLOGICAL SETTING

The Neuquén Basin is perhaps the best-known sedimentary basin in northwestern Patagonia, with abundant occurrences of terrestrial and marine fossils. This basin extends from the active magmatic arc along the Andes to the west and the Sierra Pintada System and the North Patagonian Massif to the northeast and southeast, respectively. It covers an area of over 120,000 km^2 and comprises a nearly continuous record of up to 6,000 m of stratigraphic thickness from the late Triassic to the early Cenozoic (Schwarz, 2012). Within the thick Mesozoic succession, several different orders of cyclicity are recorded, including marine and continental deposits related to transgressive-regressive episodes (Digregorio & Uliana, 1980). The sedimentary record includes continental and marine siliciclastics, carbonates, and evaporites accumulated under a variety of basin styles, including syn-rift, post-rift sag, and foreland phases (Legarreta & Uliana, 1991; Howell *et al.*, 2005). It should be noted that the fluvial design can vary throughout the basin depending on the paleotopography; however, the variation in carrying capacity is perceptible in diverse outcrops distributed throughout the Neuquén Basin (Filippi, 2021). The latter is what makes it possible to establish correlations at the regional level. The Upper Cretaceous strata of these sequences correspond to the Neuquén and Malargüe groups and are included in the Riograndic Cycle (Legarreta & Gulisano, 1989). The Neuquén Group (lower Cenomanian-middle Campanian) constitutes a sequence of continental sediments deposited during the initial foreland stage of the Neuquén Basin (Franzese *et al.*, 2003). It is the richest dinosaur-bearing unit of the basin, which includes sauropods, ornithopods, and theropods, as well as other vertebrate groups (Leanza *et al.*, 2004). Lithologically, this group comprises a succession of sandstones, conglomerates, and claystones, which represent alluvial fans, fluvial systems, and *playa*-lake environments, stacked in recurrent fining-upward sequences (Leanza & Hugo, 2001). The Neuquén Group is composed—from bottom to top—of the Río Limay, the

Río Neuquén, and the Río Colorado (Cazau & Uliana, 1973) subgroups (Ramos, 1981). The current lithostratigraphic model of the Neuquén Group proposed by Garrido (2010) divides these subgroups into seven formations according to the following scheme: Río Limay Subgroup (Candeleros and Huincul formations); Río Neuquén Subgroup (Cerro Lisandro, Portezuelo, Los Bastos, Sierra Barrosa, and Plottier formations), and Río Colorado Subgroup (Bajo de la Carpa and Anacleto formations).

In particular, the Sierra Barrosa Formation is composed of a succession of yellowish sandstones of variable granulometry with intercalations of thin mudstone levels. The type locality is situated on the meridional foothills of Sierra Barrosa and east of Cerro Challacó (Garrido, 2010). According to Herrero Ducloux (1938), in the Sierra Barrosa sector, the equivalent strata called 'Upper Portezuelo' had a thickness of around 70 m, while in its type locality its average thickness is 62 m, decreasing to 40 m in the area of Cerro Challacó (Garrido, 2010). Based on its stratigraphic relationships, a relative Coniacian age for this unit is inferred (Garrido, 2010).

Regarding the fossil record of the Sierra Barrosa Formation, around the city of Rincón de los Sauces, it is represented, until now, by materials from two sites: Loma de los Jotes, from which remains belonging to more than one sauropod individual are known (*i.e.*, MAU-Pv-LJ 471, 472 and 611), and Cañadón Mistringa, with cranial, axial and appendicular elements of a single sauropod specimen identified as *Kaijutitan maui* (*i.e.*, MAU-Pv-CM-522; Filippi *et al.*, 2019), the subject of this contribution.

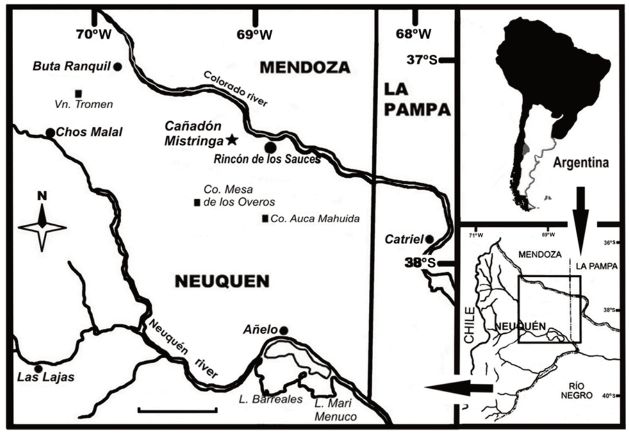

Figure 1. Location map of the Cañadón Mistringa site, Neuquén Province, Argentina. The star symbol indicates the provenance of the holotype of ***Kaijutitan maui*** (**MAU-Pv-CM-522**).

Paleoenvironmental setting

The Cañadón Mistringa site (37° 23′ 31.4″ S, 69° 01′ 07.8″ W) is located about 9 km southwest of Rincón de los Sauces locality, Pehuenches Department, Neuquén Province (Fig. 1). The *Kaijutitan* bones were found on the right margin of the canyon in outcrops of the Sierra Barrosa Formation about 5 m below the contact with the Plottier Formation (Fig. 2). The fossiliferous site is located in an area of badlands, where small gullies develop with ephemeral drainage, dumping their waters into the middle section of the Cañadón Mistringa. Along the canyon, deposits corresponding to the Sierra Barrosa Formation crop out. These are composed of thick levels of fine- to medium-grained sandstones, forming bodies of large amalgamated channels. These channel levels can reach a thickness of up to 12 m with a predominance of tractive primary sedimentary structures, developed mainly in a low flow regime. However, the channel bases are usually markedly erosive and show intraconglomerate bodies with pelitic intraclasts up to 25 cm long on their major axis. These attributes would indicate conditions of moderate energy, with exceptional periods of high to very high energy, so it is inferred that they correspond to the main channels. Towards the upper section of the succession, there is evidence of a gradual dominance of fine facies corresponding to floodplains, within which the remains studied here were found.

The fossiliferous levels are characterized by a monotonous succession of massive and reddish mudstones, in which thin horizons (less than 5 cm of thickness) alternate with greenish limestones and tabular sandy bodies (less than 12 cm of thickness). These horizons are characterized by the presence of ondulitic lamination, horizontal stratification and/or low-angle cross-stratification, which were sedimented in a floodplain environment.

MATERIAL AND METHODS

Fieldworks

The *Kaijutitan* remains were recovered within an area of approximately 20 m^2 at the Cañadón Mistringa site, and there were no duplicated elements. The 34 skeletal elements correspond to a single sauropod dinosaur specimen, these elements are of the appropriate size and morphology to belong to a single skeleton. *Kaijutitan maui* (MAU-Pv-CM-522) was recovered during successive excavations carried out between 2012 and 2018. The recovered materials include cranial, axial, and appendicular bones, as well indeterminate fragments.

Standard procedures and protocols for taphonomic data collection (Behrensmeyer, 1978, 1991) were employed during mapping and *in situ* data collection. Prepared specimens were examined macro- and microscopically to evaluate the degree of taphonomic modification. The methodology and taphonomic attributes used generally follow those of Alcalá (1994). For each bone, the following features were considered: anatomical determination, degrees of weathering, abrasion, articulation to other bones, integrity, and breakage.

Microscopic analysis

Histological features were studied through thin sections following the techniques outlined by Chinsamy & Raath (1992) and Cerda *et al.* (2020). The preparation of the histological sections (cervical and dorsal ribs, ulna, and undetermined bone) was carried out in the cutting laboratory directed by Geol. Ricardo Ponti (Buenos Aires, Argentina) and in the laboratory of Museo Carlos Ameghino (Cipolletti, Río Negro). The samples were observed under normal and polarized light with a petrographic microscope Bestscope B 5080 and under a binocular loupe Arcano ZTX 745. Images were taken with a 16MP Kodak Pixpro FZ41 digital camera. Histological terminology and definitions generally follow those of Francillon-Vieillot *et al.* (1990), Reid (1996), and Chinsamy-Turan (2005).

Institutional abbreviations. MAU-Pv-CM, Museo Municipal Argentino Urquiza, Paleontología de Vertebrados, Cañadón Mistringa, Neuquén, Argentina.

Histological and diagenetic abbreviations. EFS, external fundamental system; **FLB,** fibrolamellar bone; **HB,** Haversian bone; **HOS,** Histologic ontogenetic stages; **LAGs,** lines of arrested growth.

BIOSTRATINOMY

Integrity and skeletal representation

The outcrop of the Sierra Barrosa Formation is exposed in the Cañadón Mistringa site (Fig. 2), where very large remains of an individual were found (~30 m length), identified as *Kaijutitan maui* (Filippi *et al.*, 2019). The degree of integrity was evaluated following the categories proposed by Alcalá (1994): 0: complete bone, 1: incomplete bone. Of all the bones recovered at the site, the smallest proportion of them (26%) are complete, such as one anterior cervical vertebra, the left ulna, the II right metacarpal, the III right metacarpal, the right tibia, and the left astragalus; while the majority of the bones found (74%) are incomplete (Tab. 1). The *Kaijutitan* specimen comprises the incomplete neurocranium, two cervical vertebrae, one caudal vertebra, three incomplete cervical ribs, four incomplete dorsal ribs, the incomplete shoulder girdle, 11 limb bones, one incomplete left ilium, and 8 indeterminate bones (Tab. 1). There is no zonal and differentiated distribution in the site regarding complete and incomplete elements, but these are mixed as seen in the taphonomic map (Fig. 3).

Articulation, orientation, and dispersion

The *Kaijutitan* specimen was preserved in the horizontal plane on the bedding surface. The bones were found in two levels (numbered 1 and 2). Level 1, from which most of the bones come, is located approximately 30 cm below level 2 (Fig. 3). No lithological difference or discontinuity is observed between level 1 and level 2. In both fossiliferous levels, we recognized the articulation degrees proposed by Behrensmeyer (1991): (1) disarticulated-associated elements comprised by the neurocranium, one anterior cervical vertebra, right humerus, right ulna, right radius, II right metacarpal, III right metacarpal, left sternal plate, left coracoid, left scapula, ?left humerus, left ulna, right femur, right tibia, and three dorsal ribs; (2) associated-scattered elements which include one anterior caudal vertebra, the right distal epiphysis of metatarsal II, a left ilium fragment, and the left astragalus.

The geological data collected in the fossiliferous site allowed to determine the absence of paleocurrents. It should be noted that, in the vicinity of the paleontological site, the main channels indicate an average orientation of

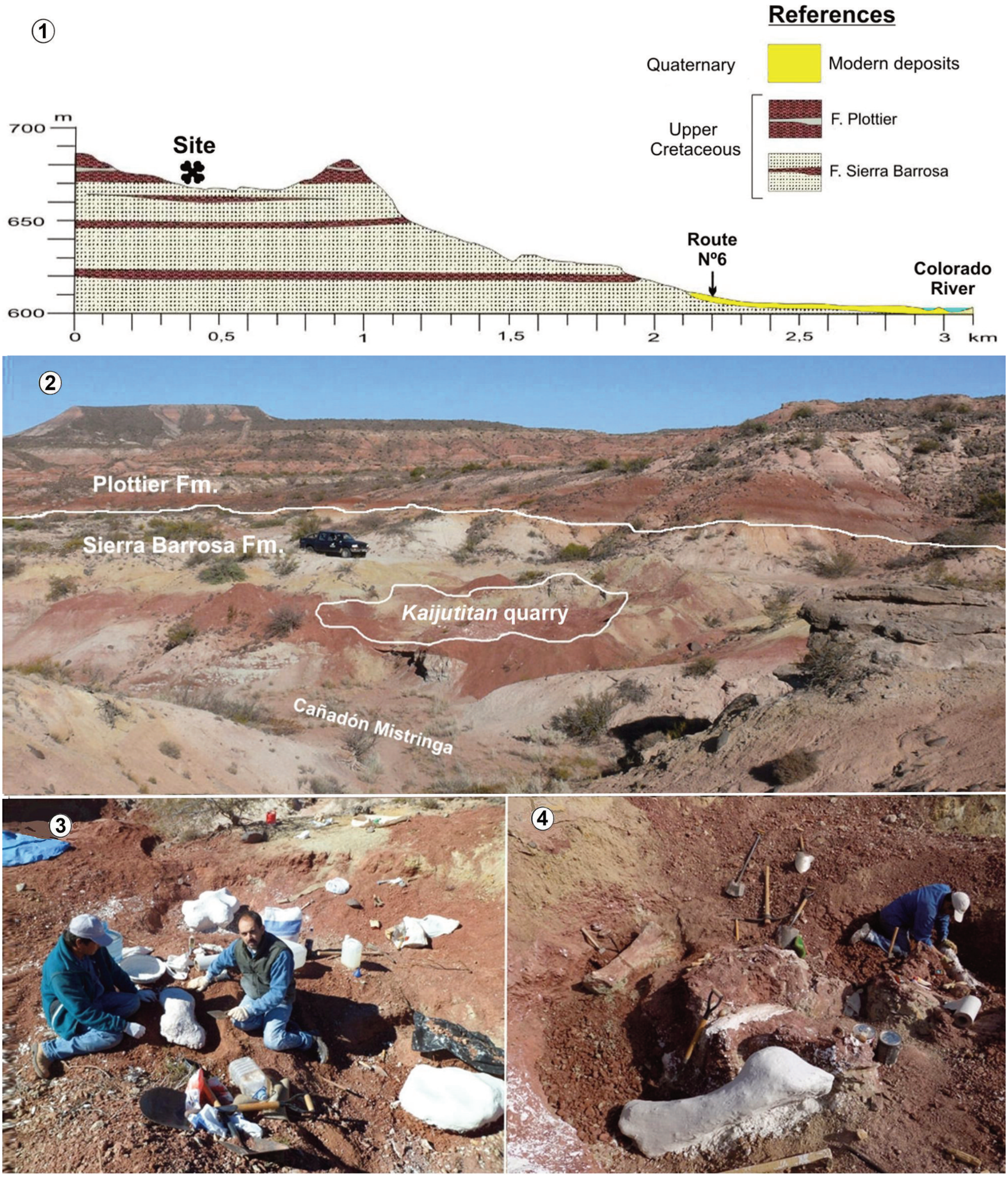

Figure 2. 1, Geological section of the area where ***Kaijutitan*** **(MAU-Pv-CM-522)** was found. **2,** General view of the ***Kaijutitan*** site showing the contact between the Plottier and Sierra Barrosa formations; **3–4,** images were taken during the fieldworks.

TABLE 1- Taphonomic attributes of the *Kaijutitan maui* specimen examined (N=34)

Taphonomic Attributes	Category	Percentage ratio %
Integrity		
Complete	0	26%
Incomplete	1	74%
Weathering		
Intact bone	1	65%
Superficial bone loss	2	20%
Deep bone loss	3	15%
Abrasion		
Intact bone	1	65%
Rounded bone	2	29%
Polished bone	3	6%
Number of breakage		
Bone with a fracture	1	3%
Bone with two fractures	2	–
Bone with more than two fractures	3	97%
Type of breakage		
Bone broken by manipulation	2	–
Bone with transverse fractures	3	42%
Bone with oblique fractures	4	31%
Bone with parallel fractures	5	27%

310° NW. All the recovered bones were found in a horizontal or sub-horizontal position, with the exception of the left sternal plate (17, Fig. 3) which rested on its medial edge; the humerus (18, Fig. 3) was inclined approximately 40°, and the radius (21, Fig. 3) was in an almost vertical position; these last two bones rested on their distal ends. The spatial distribution of the bones respects the relative position and configuration of the body plan of the specimen and shows the accumulation of the largest remains located in the SW sector of the excavation (Fig. 3).

Weathering degree

Weathering is defined by Behrensmeyer (1978) as the process by which the original microscopic organic and inorganic components of a bone are separated from each other and destroyed by physical and chemical agents operating on the bone *in situ*, either on the surface or within the soil zone. According to this definition, physical damage caused by carnivore mastication, trampling, fluvial transport, and geochemical changes which take place diagenetically during fossilization are excluded from consideration, although such processes are close to weathering.

Alcalá (1994), based on the stages of weathering proposed previously by Behrensmeyer (1978) about observations of recent bones in Amboseli Park, Kenya, proposed three weathering categories for the analysis of this attribute in fossil remains of large vertebrates. For this reason, the categories proposed by Alcalá (1994) were considered here: (1) intact bone (without any alteration);

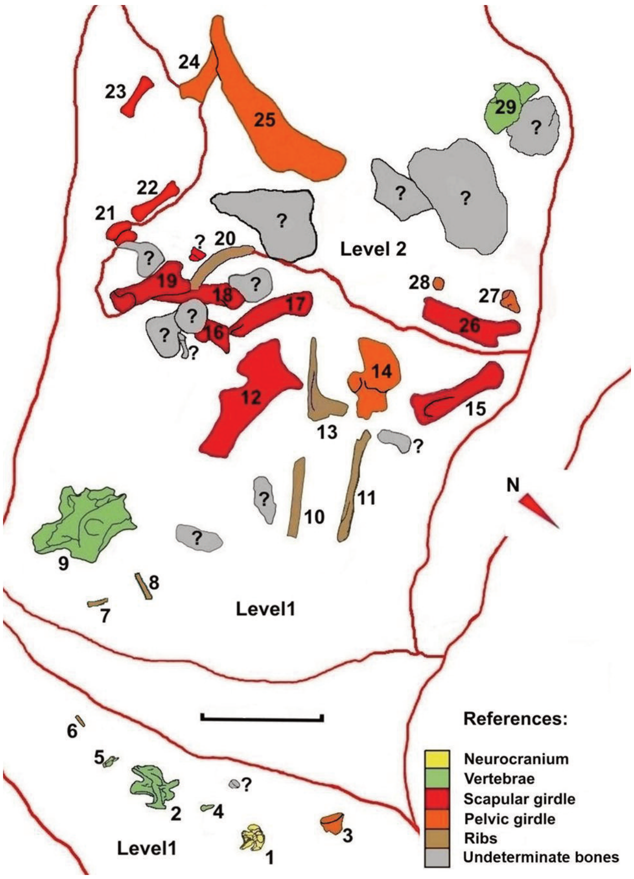

Figure 3. Taphonomic map of the ***Kaijutitan*** quarry. List of recovered bones: **1,** neurocranium; **2,** anterior cervical vertebra; **3,** metatarsal II; **4,** fragment of ?prezygapophysis; **5,** fragment of dorsal prezygapophysis?; **6–8,** cervical ribs; **9,** posterior cervical vertebra; **10 and 11,** dorsal ribs; **12,** left scapula; **13,** dorsal rib; **14,** right ilium; **15,** right ulna; **16,** right coracoid; **17,** left sternal plate; **18,** left humerus; **19,** left ulna; **20,** dorsal rib; **21,** left radius; **22 and 23,** left metacarpals; **24,** right tibia; **25,** right femur; **26,** right humerus; **27,** right talus; **28,** ?calcaneus; **29,** anterior caudal vertebra. Red lines correspond to the excavation area. (Note: undetermined bones were not listed). Scale bar= 1 m.

(2) remains showing surface loss of compact bone; and (3) remains showing deep loss of bone material, affecting spongy tissue (Fig. 4; Tab. 1).

Most of the elements of level 1 (65%) are well-preserved, that is, they show intact bone (category 1); 20% are included in category 2; and the remaining 15% are poorly-preserved, including a posterior cervical vertebra, the left scapula, and a left ilium fragment (category 3).

Most of the bones preserved in level 2 (*e.g.*, right tibia and the left astragalus) are well-preserved; while 15% show a higher degree of weathering (category 3). In some remains from level 2, such as the ?left humerus, there is also clear evidence of differential weathering (Rogers, 1990; Casal *et al.*, 2023), a process that occurs when half of the bone is buried and the other half is exposed to the surface (Fig. 4.5–7; Tab. 1).

Some particular cases include: left ulna and scapula with transverse fractures and longitudinal cracking parallel to bone fibers, generating a mosaic pattern (stage 2 of Behrensmeyer, 1978). This pattern is very visible in the diaphyseal region of the left ulna and in the scapula (Fig. 4.11–12).

Abrasion degree

The abrasion is the wear process that generates the smoothing of the edges and vertices of the bones (*sensu* Shipman, 1981), whose consequence is the loss of surface irregularities and/or acquisition of a spherical shape (Alcalá, 1994). This attribute was determined following the categories proposed by Alcalá (1994) for both micro- and macro-elements: (1) intact bone; (2) rounded bone; and (3) polished bone (Fig. 4; Tab. 1). There is no difference in abrasion between levels 1 and 2. The 65% of the recovered elements are intact (category 1). The remaining elements (35%) correspond to bones with evidence of abrasion, of which 29% belong to category 2 and 6% to category 3. Category 2 includes the neurocranium, which presents the left paraoccipital process with rounded edges; the anterior cervical vertebra with a wear condyle and zygapophyses; the worn articular surfaces of metacarpal II; the astragalus; and several indeterminate rounded bones. Category 3 includes the posterior cervical vertebra, which presents its entire surface extremely eroded, and the ?left humerus, which present the posterior half of the diaphysis eroded and worn, exposing the spongy tissue (Fig. 4.5–7).

Number and types of breakage

The number of fractures presented by the bones was considered according to Alcalá (1994). The 3% of the preserved elements show a single fracture, while the remaining 97% present more than two fractures (Tab. 1).

The analysis of the types of fractures was performed in long bones (*sensu* Alcalá, 1994; Tomassini *et al.*, 2010). It was established on the basis of the angle formed by the

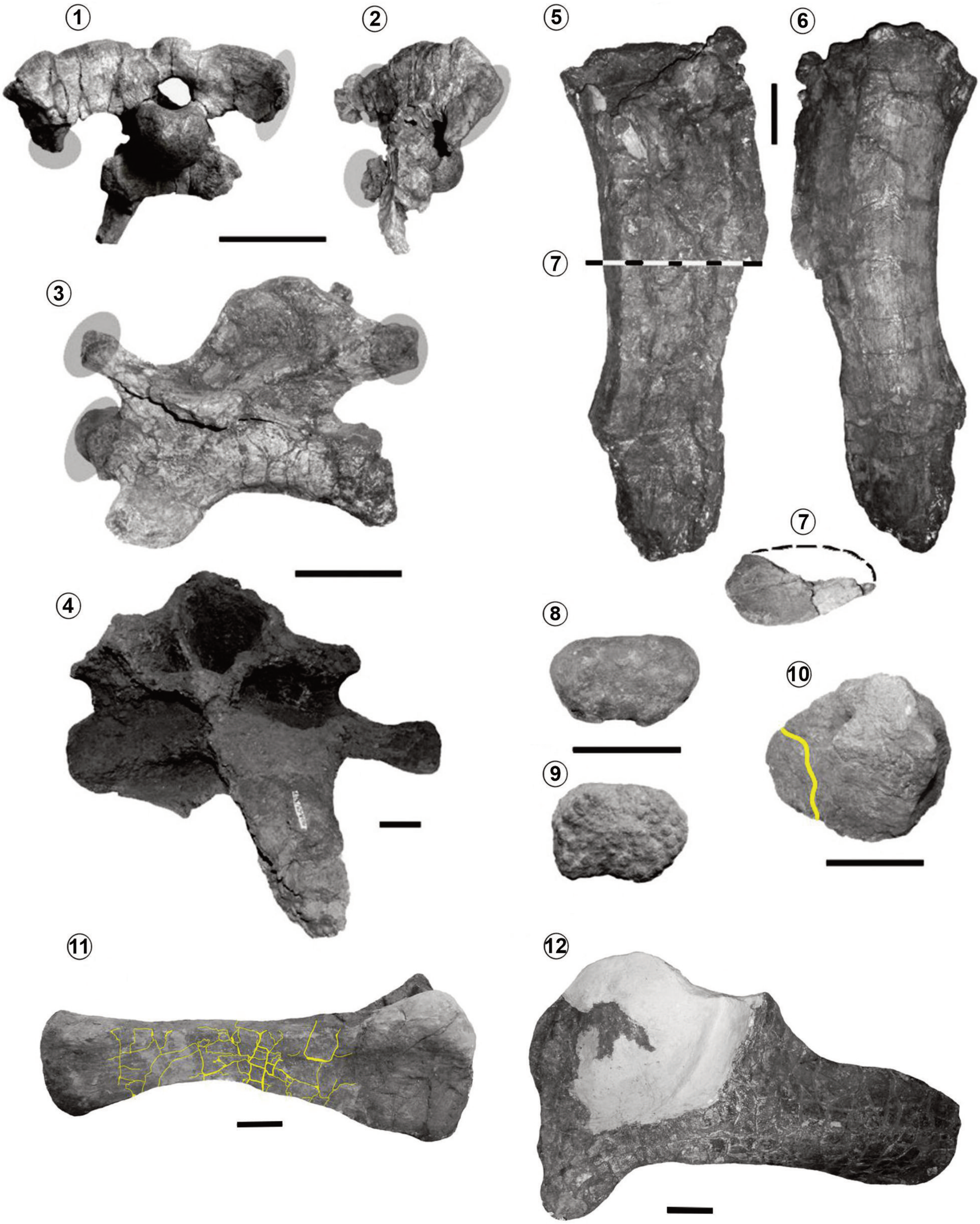

Figure 4. Cranial and postcranial elements of ***Kaijutitan*** (**MAU-Pv-CM-522**) with evidence of abrasion. **1,** skull in posterior and **2,** lateral view; **3,** anterior cervical vertebra and **4,** posterior cervical vertebra**,** in lateral view; **5,** ?left humerus in anterior**, 6,** posterior, and **7,** cross-sectional views; **8,** metacarpal II, and **9,** metacarpal III, in distal view; **10,** astragalus in proximal view; **11,** left ulna in medial view and **12,** left scapula in lateral view**.** The gray ovals show the sectors where there is evidence of abrasion; the main fracture of the astragalus is shown in yellow, and the dashed line of left humerus indicates the position of a transverse fracture. The anterior cervical **(3),** ?left humerus **(5–7)** and metacarpals II **(8)** shows evidence of weathering, while left ulna **(11)** and scapula **(12)** show evidence of cracking. Scale bar= 10 cm.

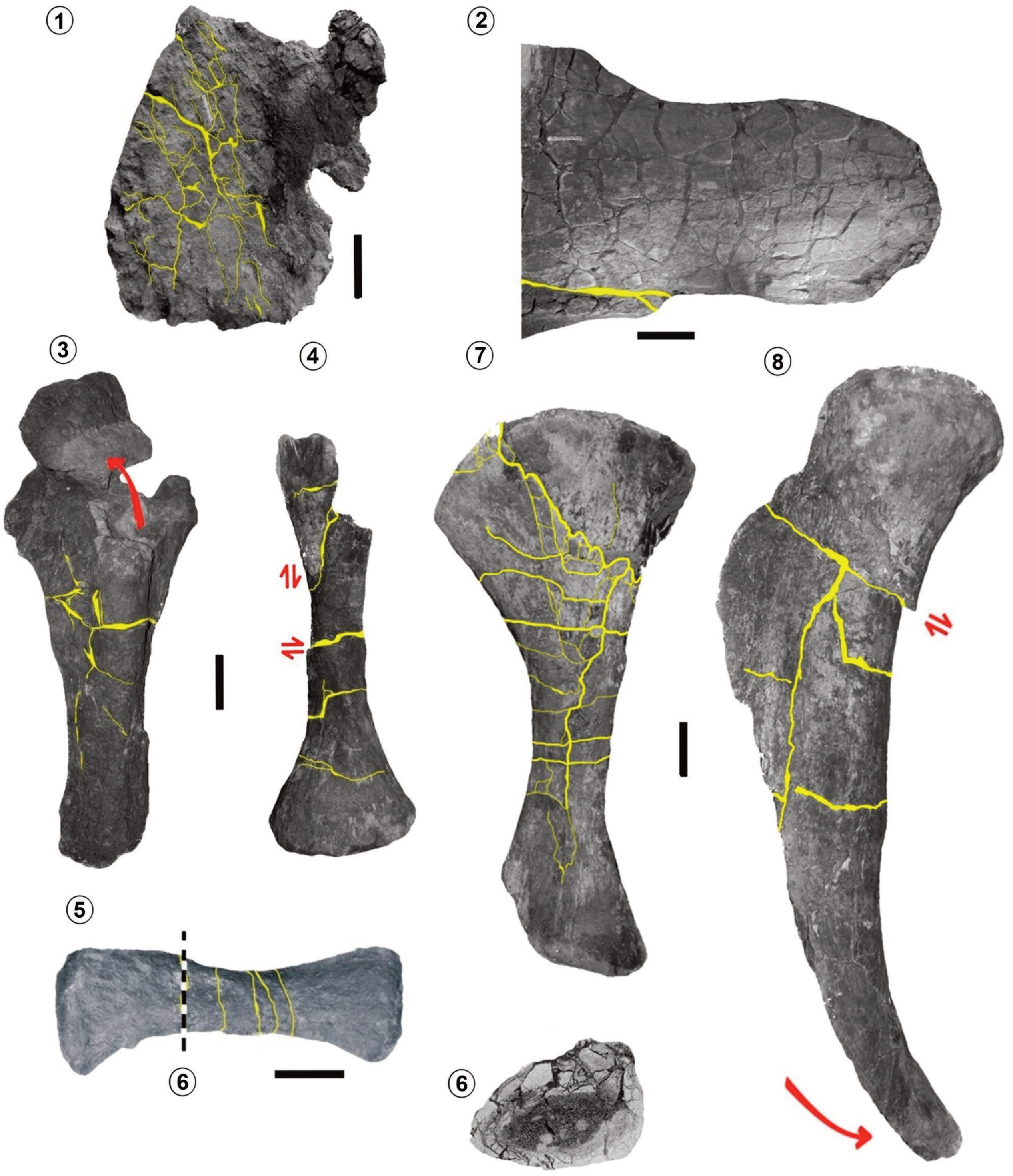

Figure 5. Elements of the scapular girdle, forelimb, and hindlimb of ***Kaijutitan*** (**MAU-Pv-CM-522**) with evidence of fractures and displacements. **1,** left coracoid in lateral view; **2,** preserved portion of the left scapular blade in lateral view; **3,** right ulna in medial view; **4,** right radius in posterior view; **5,** right metacarpal II, in anterior view; and **6,** fracture in transverse view; **7,** right tibia in medial view; **8,** right femur in anterior view. The red arrows show the direction of shear and displacement fractures, the main fractures are shown in yellow, and the dashed line shows the position of the transverse fracture in metacarpal II. Scale bar= 10 cm.

main dimension axis and the border of fracture; longitudinal (0°–29°), oblique (30°–59°) and transverse (60°–90°) fractures were considered (Tab. 1). The 42% of bones have transverse fractures (category 3), these being the most common type, whereas 31% of bones have oblique fractures (category 4) and 27% of the bones recorded had longitudinal fractures parallel to the longitudinal axis of the element (category 5) (Figs. 5 and 6; Tab. 1). The right ulna (Fig. 5.3) has the proximal end displaced, while the distal end was not preserved. The right radius (Fig. 5.4) shows displacement or shear fractures, particularly in the mid-diaphysis. The right metacarpal II (Fig. 5.5–6) exhibits multiple cemented fractures with different angles and directions. The right tibia (Fig. 5.7) presents longitudinal and transverse fractures and an oblique fracture that displaces the proximal epiphysis. The right femur (Fig. 5.8) shows an oblique shear fracture in the proximal sector, which generated a displacement in the internal face of the epiphysis, in addition to several transverse fractures that were later cemented by calcite in fossil-diagenetic stages. The distal end of the femur displays a curvature on its internal face as a consequence of plastic deformation.

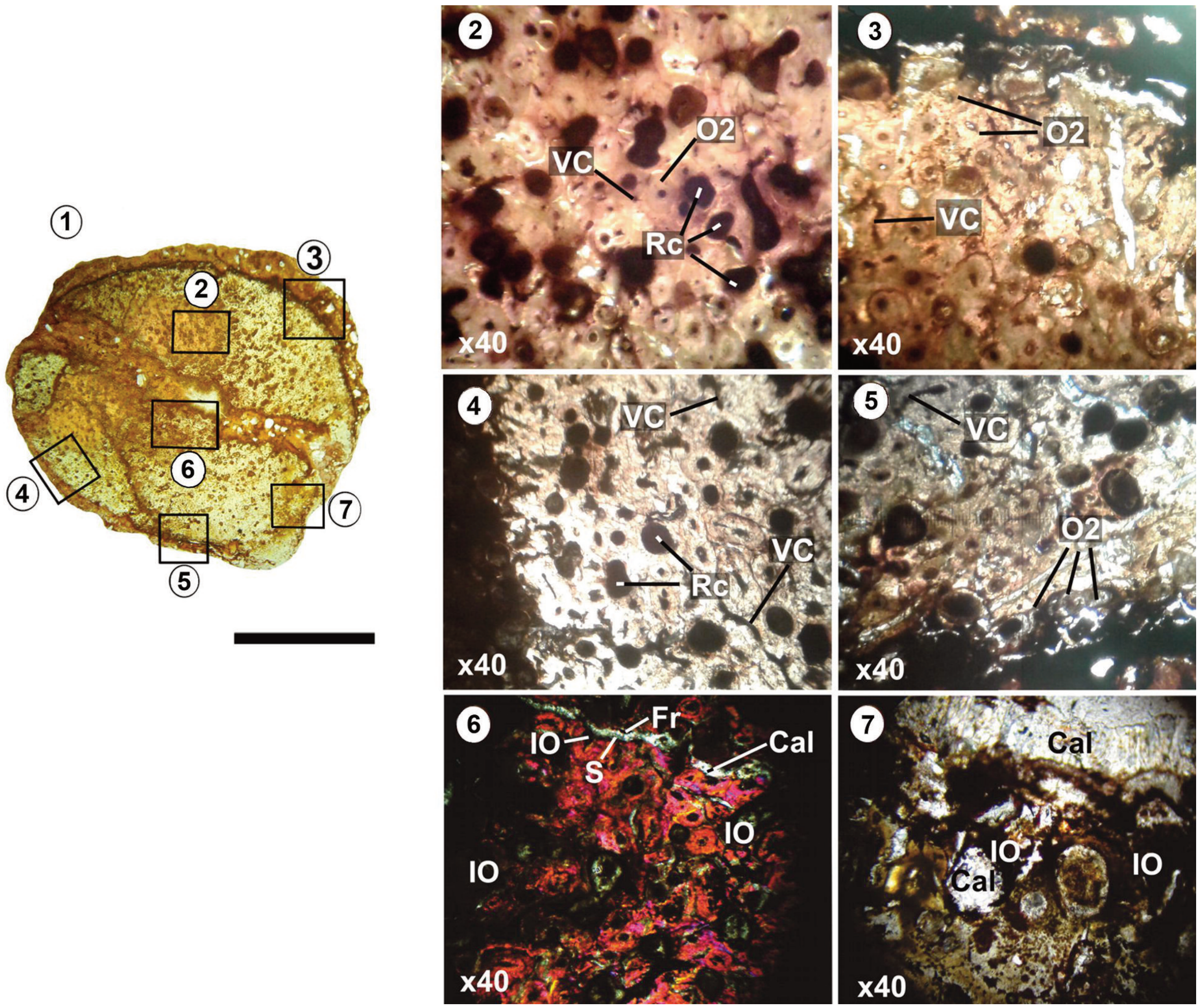

Figure 6. MAU-Ph-CM-020. Cervical rib of ***Kaijutitan***. **1,** cross section of the sample; **2,** Haversian tissue of the deep cortex with secondary osteons, Volkmann's canals, and resorption cavities; **3–5,** Haversian tissue from different sectors of the cortex; **6,** vascular canals, secondary osteons, and fractures filled by sediment, iron oxides, and calcite; **7,** fibrous calcite cementation in the cortical wall. Abbreviations: **Cal**=calcite; **IO**=iron oxide; **Fr**=fracture; **OS**=secondary osteons; **Rc**=resorption cavities; **S**=sediment; **VC**=Volkmann canal. Photomicrographs in normal light **(2, 3, 6)** and polarized light with lambda filter **(4, 5, 7).** See text for further explanation. Scale bar= 10 mm.

BONE MICROSTRUCTURE AND DIAGENESIS

Cervical rib MAU-Ph-CM-020

The sample analyzed consists of a cervical rib fragment in complete cross section showing a notorious midline fracture filled by sediment (Fig. 6.1). It shows entirely compact bone with a high degree of secondary remodeling. The Haversian bone displays a high density of longitudinally oriented secondary osteons, easily distinguishable by the presence of cement lines and connected by Volkmann's canals, as well as visible resorption cavities (Fig. 6.2–5). Secondary osteons develop in the outermost layer of the cortex, which has an irregularly contoured surface. These osteons are the result of a process of secondary reconstruction, involving the removal of bone around a primary vascular canal, followed by subsequent redeposition of concentrically arranged lamellar bone in the erosion cavity (Chinsamy, 1997). There is no evidence of LAGs, zones, or annuli.

The bone tissue of the rib shows compaction and late-diagenesis distortion (Fig. 6.4–5). Vascular canals and osteons are mainly filled with sediment, iron oxides, and calcite ($CaCO_3$). Thin laminae of the sediment and iron oxide infiltrations are occupying the edge of the fractures (Fig. 6.6). Occasionally, the iron oxides are not entirely filling the osteonal spaces, leaving space that is filled by drusy calcite mosaics (Fig. 6.6). The rib has an outer calcareous crusting that suffered dissolution in some sectors favoring fibrous calcite cementation (Fig. 6.7).

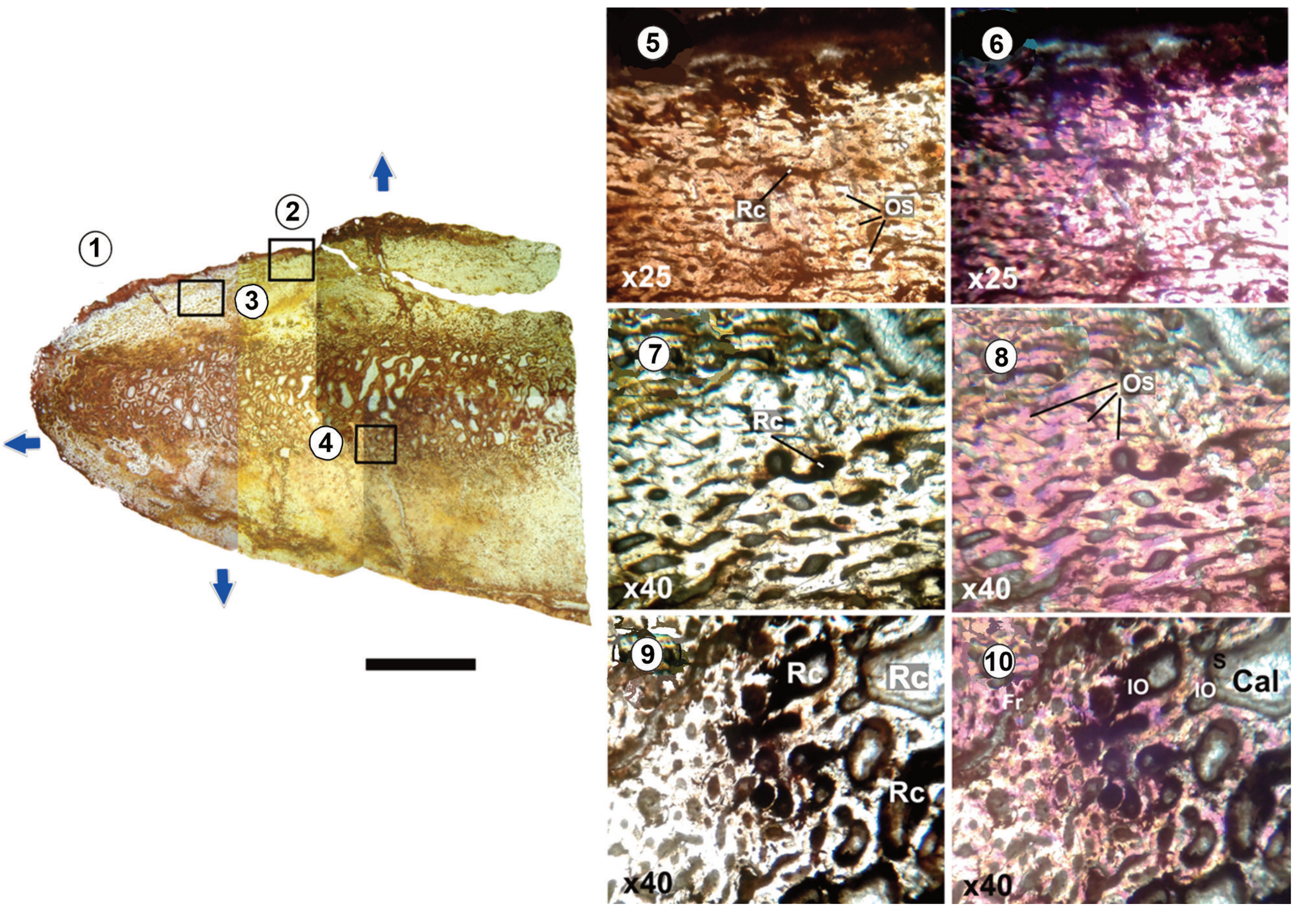

Figure 7. MAU-Ph-CM-017. Dorsal rib of ***Kaijutitan***. **1,** cross section of the sample; **2,** The cortical region showing Haversian tissue with secondary osteons and resorption cavities **(5–6)**; **3,** Haversian bone of the deep cortex **(7–8)**; **4,** medullary region showing spongy tissue; **9-10,** detail of trabeculae, resorption cavities and fractures filled by sediment, iron oxides, and calcite. The blue arrow indicates the external surface of the bone. Abbreviations: **Cal**=calcite; **IO**=iron oxide; **OS**=secondary osteons; **Rc**=resorption cavities; **S**=sediment. Photomicrographs in normal light (**5, 7, 9)** and polarized light with lambda filter (**6, 8, 10).** See text for further explanation. Scale bar= 10 mm.

Dorsal rib MAU-Ph-CM-017

This sample corresponds to the mid-distal portion of an anterior dorsal rib. The cross section shows a subelliptic contour in which two well-differentiated regions of tissue are observed: an external compact cortical bone and a central spongy tissue (Fig. 7.1). The cortical tissue is composed of compact bone that has undergone, as in the cervical rib, a high degree of bone remodeling with secondary osteons reaching to the outermost layer of the cortical surface (Fig. 7.2–3). In the inner cortex, although the density of secondary osteons is abundant, resorption cavities increase towards the medullary region (Fig. 7.3). There is no evidence of growth marks. Trabecular tissue and wide resorption cavities are observed in the medullary region (Fig. 7.4).

The rib microstructure displays different episodes of mineralization (Fig. 7.2–4). The cortical region shows

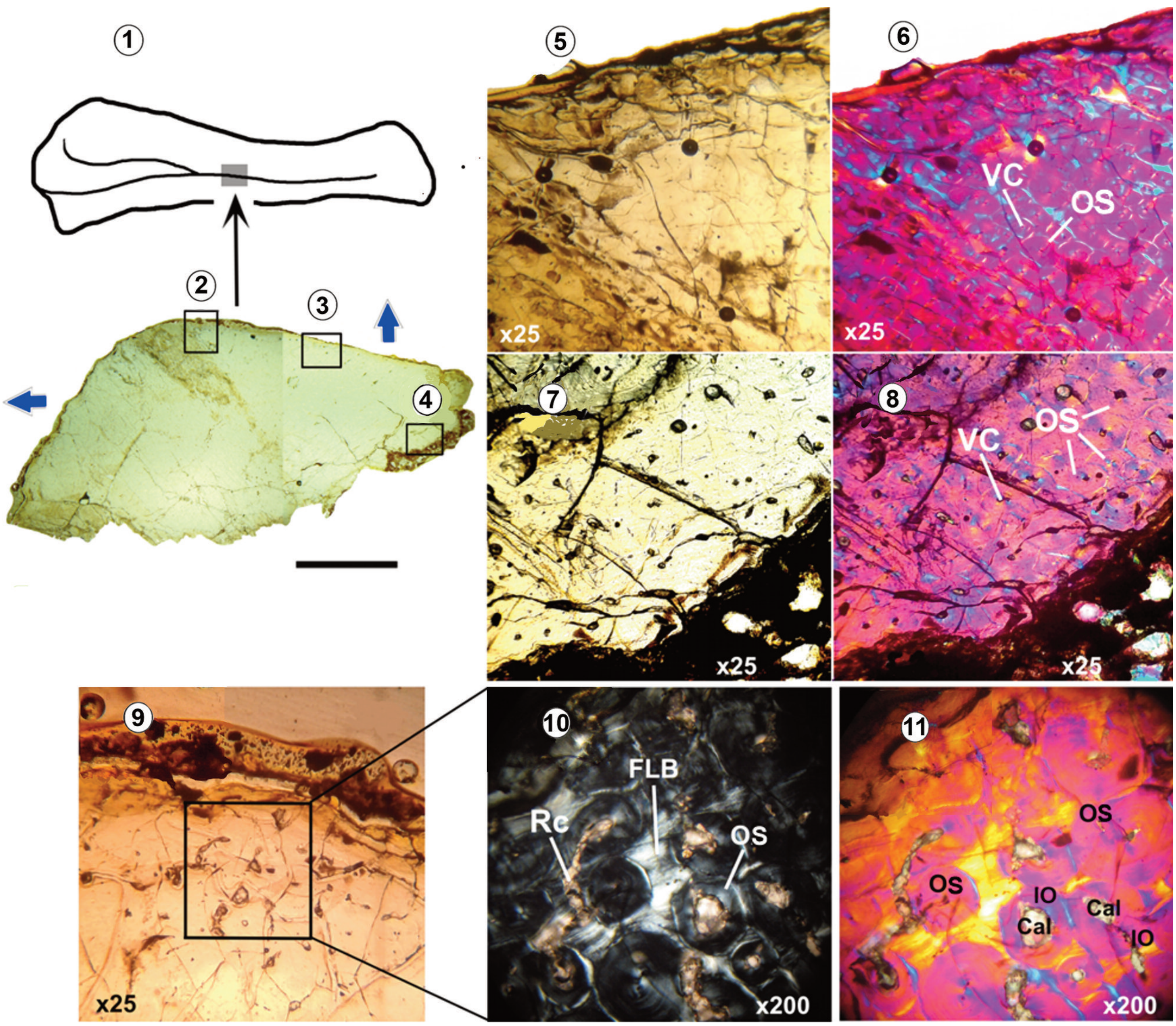

Figure 8. MAU-Ph-CM-018. 1, Left ulna cortical fragment of ***Kaijutitan***, with cross section of the sample; **2 (5–6)** and **3 (7–8).** The Haversian bone showing high degree of secondary remodeling with secondary osteons connected by Volkmann's canals; **4.** Haversian dense reconstruction with secondary osteons, **9,** detail of inset in **10,** showing fibrolamellar tissue in some interstices between the secondary osteons; **11,** Haversian and Volkmann's canals are filled by iron oxides and calcite. The blue arrow indicates the external surface of the bone. Abbreviations: **FLB**=fibrolamellar bone; **Cal**=calcite; **IO**=iron oxide; **OS**=secondary osteons; **Rc**=resorption cavities; **VC**=Volkmann canal. Photomicrographs in normal light **(5, 7, 10),** polarized light with lambda filter **(6, 8, 10),** and cross-polarized light **(11).** See text for further explanation. Scale bar= 10 mm.

precipitation of iron oxides in vascular canals, secondary osteons, and fractures. The medullary cavity contains trabeculae and resorption cavities filled by sediment and blocky calcite, with high iron content (Fig. 7.10).

Left ulna MAU-Ph-CM-018

The sample comprises a cortical portion of the anteromedial border of the left ulna, close to the middle of the diaphysis (Fig. 8.1). The cross section shows compact bone with a high degree of secondary remodeling. The dense Haversian reconstruction is recognized by well-developed secondary osteons (Sander, 2000) (Fig. 8.2–3). Unremodeled primary bone is formed by fibrolamellar complex (Fig. 8.10). Secondary osteons are seen up to the outermost layer of the cortical surface. Resorption cavities are scarce. There are no LAGs, zones, or annuli.

The microstructure reveals that the main diagenetic processes affecting the bone were permineralization, compaction, and deformation (Fig. 8.2–4). The thin section (Fig. 8.3) displays microcracking and fractures superimposed onto secondary osteons cemented by iron oxides. The ulna has outer crusting composed of the host rock sediment and was cemented by iron oxides and calcite (Fig. 8.3). Haversian and Volkmann's canals are filled by initial precipitation of iron oxides followed by calcite cementation (Fig. 8.11).

Bone fragment MAU-Ph-CM-019

This element constitutes a cross section of an indeterminate bone which was only used to evaluate its anatomical assignment (Fig. 9.1). The sample consists entirely of spongy tissue with a very dense network of trabeculae made up of lamellar tissue, between which wide inter-trabecular spaces are observed. No compact cortical tissue is observed in any sector of the sample. Due to this, it was not possible to establish its osteological nature. This incomplete element, as well as other remains preliminarily interpreted as osteoderms, probably correspond to bones that have been diagenetically altered.

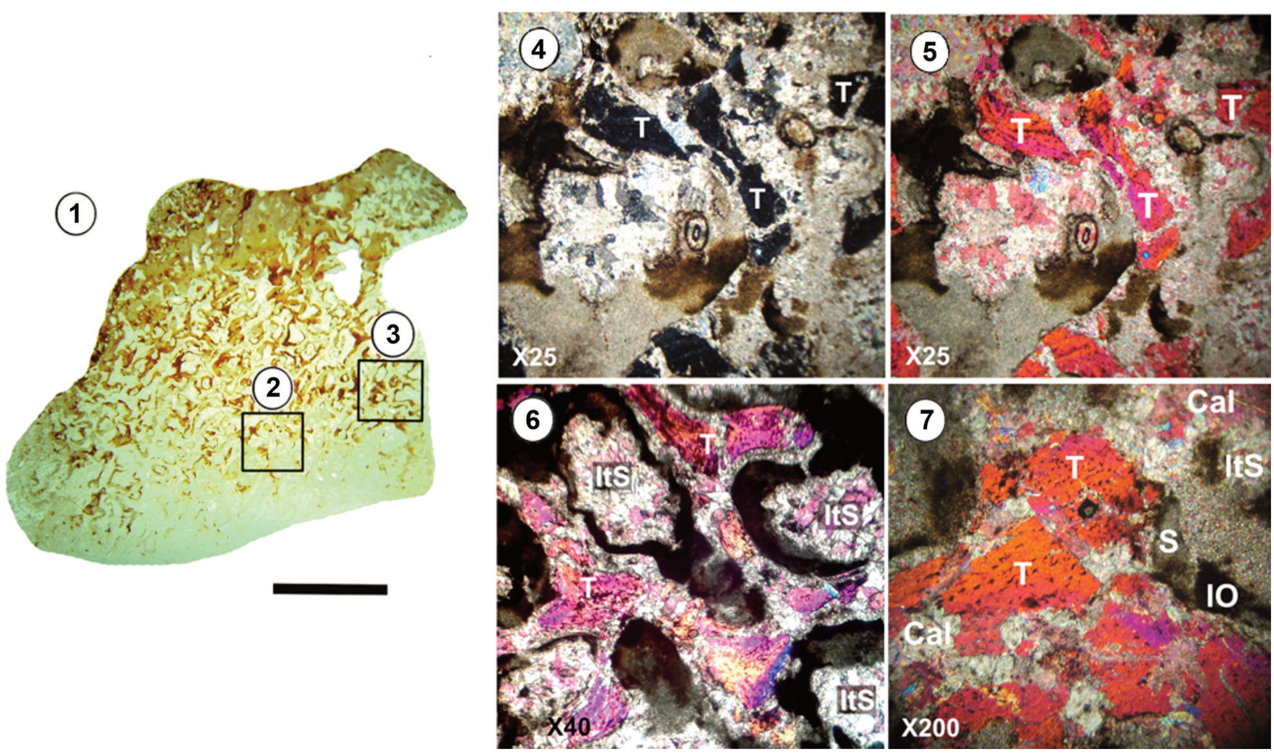

Figure 9. MAU-Ph-CM-019. Undeterminate bone fragment of ***Kaijutitan***. **1,** cross section of the sample; **2 (4–5),** cancellous tissue showing trabeculae and intertrabecular spaces; **3 (6),** spongy medullary tissue filled by drusy calcite mosaics; **7,** detail of trabeculae and inter-trabecular spaces filled by sediment, iron oxides and calcite. Abbreviations: **Cal**=calcite; **IO**=iron oxide; **ItS**=inter-trabecular spaces; **S**=sediment; **T**=trabeculae. Photomicrographs in normal light **(4)** and polarized light with lambda filter **(5, 6, 7).** See text for further explanation. Scale bar= 10 mm.

The spongy bone displays trabeculae and inter-trabecular spaces with sediment and iron oxides infiltrations forming the first generation of infills. The calcium carbonate cement occupied the inner parts of inter-trabecular spaces forming the second generation of infills (Fig. 9.3,6,7). Drusy calcite mosaics fill the centers of spaces between trabeculae, forming the third generation of infills (Fig. 9.3,6,7).

DISCUSSION

Biostratinomic pathway

In floodplains environment from the Sierra Barrosa Formation in the Cañadón Mistringa site, mostly disarticulated associated bones corresponding to titanosaur *Kaijutitan maui* were found (Filippi *et al.*, 2019). Unfortunately, no information is available on the orientation of each bone from the excavation; however, the general mapping of elements showed a generalized dispersion.

In addition, taking into account that in order to move the bones of large extant mammals such as hippopotamuses, elephants, or rhinoceroses (in this case, sauropods, whose bones are even larger), strong currents would be necessary, like those that occur in flooding events (Behrensmeyer, 1975). Therefore, this allows us to determine that the recorded orientation and dispersion of the elements recovered from *Kaijutitan* would not have occurred mainly due to fluvial action.

On the other hand, the specimen was preserved with its elements largely respecting its original anatomical position. This could suggest that for a period of time, prior to the final position of the bones before burial, the carcass of this animal remained articulated. The state of preservation of the bones suggests that some of them (*e.g.*, neurocranium, anterior cervical vertebra, metacarpals, and astragalus) suffered less subaerial exposure and therefore rapid burial in relation to most of the elements, especially those located in level 2. The difference in levels would correspond to variations in the paleo-relief. Elements from level 2, on the contrary, experienced strong weathering due to longer subaerial exposure and the action of possible scavengers on the carcass that acted as dispersing agents in the site during the biostratinomic stage (*e.g.*, Buffetaut & Suteethorn, 1989; Erickson & Olson, 1996; Chure *et al.*, 1998; among others).

For as long as the carcass was exposed on the floodplain surface, subaerial bone differential weathering occurred. The bones analyzed present different degrees of weathering (1–3 from Alcalá, 1994); however, most of them are well-preserved or have slight to moderate weathering. Long bones show longitudinal cracking, mosaic cracking, and flaking of outer surfaces (stages 1 and 2 of Behrensmeyer, 1978). Such characteristics are common in fluvial environments with episodic sedimentation, like proximal floodplains (Bridge, 2003; González Riga *et al.*, 2022; Casal *et al.*, 2023). In some bones (*e.g.*, posterior cervical vertebra, left scapula, and left ilium) the spongy tissue is exposed (stage 3 of Behrensmeyer, 1978) indicating a relatively long time of subaerial exposure before burial (Behrensmeyer, 1978; Lyman, 1994). The majority of skeletal elements do not show any evidence of abrasion; however, some elements show moderate (*e.g.*, neurocranium, anterior cervical vertebra, metacarpal II, astragalus) to intense abrasion (*e.g.*, posterior cervical vertebra, ?left humerus). The bones also present numerous perpendicular and oblique fractures, some with an irregular surface, which occurred during the diagenetic stage (Previtera, 2013). The distortions observed in a few bones occurred during the early diagenetic stages, when they still were susceptible to be plastically deformed, as consequence of soil compaction by lithostatic load inside the floodplain. Some bones are covered by an outer calcareous crust, which could be masking the existence of borings or bioerosion signals that may have affected the remains during the biostratinomic stage (Previtera, 2019).

Based on the available evidence, a possible taphonomic scenario is established for the Cañadón Mistringa site, in which the *Kaijutitan* specimen is interpreted as parautochthonous buried within its habitat with minimal disturbance, that is, not transported outside its original habitat (Kidwell *et al.*, 1986).

The apparent lack of preferred orientation of long bones (Voorhies, 1969; Behrensmeyer, 1991; Grigorescu & Csiki, 2002) within the proximal floodplain deposits of mixed-load fluvial systems indicates non-intense hydraulic processes and of short-term. However, in this proximal floodplain, a slight removal and exposure of skeletal remains occurred due to the influence of crevasse splay (González Riga &

Astini, 2007). It should be noted that there is no evidence that the bones were buried by the crevasse splay.

At the *Kaijutitan* site, two taphonomic patterns of occurrence are distinguished: skeletal elements exposed for a long period of time and another with rapidly buried remains. The bones that experienced long-term exposure are represented by scattered and disarticulated bones. This scenery is interpreted as a consequence of the probably biotic action. On the other hand, the remaining associated bones represent those buried rapidly after death (around 1–2 years *sensu* Behrensmeyer, 1978) during flooding events (Botfalvai *et al.*, 2017). The intense fragmentation of some bones could be explained by the effect produced on the carcass by biological agents, which contributed to their disarticulation and dispersion in a relatively small area. Although in the *Kaijutitan* bones there is no direct evidence of the presence of predators and scavengers (*e.g.*, bite marks, shed carnivore teeth), nevertheless, at the Loma de los Jotes site (Filippi, 2021), at stratigraphical levels of the Sierra Barrosa Formation, located approximately 4 km from the study site, theropod teeth were found associated with remains of sauropods *indet*. In support of this interpretation, recent work by Baiano & Filippi (2022) reports a new tetanuran theropod partial tibia from the same formation, increasing the theropod fauna for the Sierra Barrosa Formation that currently only included the megaraptorid *Murusraptor barrosaensis* (Coria & Currie, 2016). The occurrence of small theropods with large sauropods could suggest the presence of scavenging and breakdown of bigger remains, as has been reported elsewhere in northern Patagonia (Gonzalez Riga & Astini, 2007).

Paleobiology

The study of the bone microstructure of an organism provides information on aspects of its biology, physiology, and ontogenetic development. In dinosaurs, there are several studies that provide information on the ontogenetic stage of different taxa (Erickson *et al.*, 2004; Wings *et al.*, 2007; Company, 2011; D'Emic *et al.*, 2012; Gallina, 2012; Cerda & Chinsamy, 2012; Ibicuru *et al.*, 2013; Hendrick *et al.*, 2014; Cerda *et al.*, 2019; Cruzado-Caballero *et al.*, 2019). However, there are few that have, for the same species, more or less complete ontogenetic series that allow their ontogenetic stages to be established (Curry Rogers, 1999; Horner *et al.*, 2000; Erickson & Tumanova, 2000; Sander, 2000; Klein & Sander, 2008). Klein & Sander (2008) have established a series of HOS. They established 13 HOS, using changes in laminar FLB and in intensity of remodeling by secondary osteons (number and density) by differentiating seven bone tissue types. HOS have been used to infer the ontogenetic stage in different sauropods, like *Phuwiangosaurus* (Klein *et al.*, 2009); *Alamosaurus* (Woodward & Lehman, 2009); *Magyarosaurus* (Stein *et al.*, 2010); *Lirainosaurus* (Company, 2011); and *Bonitasaura* (Gallina, 2012).

In the present case, the elements sampled from the *Kaijutitan* specimen representing different sectors of the skeleton present a similar histological structure characterized almost entirely by the presence of dense HB, with the exception of the left ulna, in which the bone matrix is barely recognizable between the secondary osteons. Probably due to advanced bone remodeling, growth marks and other primary histologic structures were eliminated (Fig. 8.10).

On the other hand, the outer circumferential lamellae (Enlow & Brown, 1957), later called outer circumferential layer (Chinsamy-Turan, 2005); accretionary bone (Reid, 1996) formed by external avascular tissue; or EFS (Cormack, 1987) were not observed. An EFS is a peripheral layer of avascular or very poorly vascularized slowly forming bone tissue that often contains multiple closely spaced LAGs and generally indicates that skeletal growth has essentially ceased (Botha-Brink *et al.*, 2018). However, there is an important controversy over the biological meaning (sexual or skeletal maturity) of the onset of deposition of the EFS. The most significant variation in the histological features occurs within the last growth cycles before deposition of the EFS, indicating that there is an important slowdown of growth shortly before reproductive maturity. This trend could be related to the onset of physiological maturity (Jordana *et al.*, 2016).

It should be considered that diagenesis affected the preservation of most studied bones, masking the original histological characteristics. In the case of the ulna (see Fig. 8), the cortical region shows dense HB with a high degree of secondary remodeling and very little or no vascularization, which makes it possible to determine an HOS-13 (adult) for the specimen, according to Klein & Sander (2008). This is consistent with data indicating that vascularization and growth rates decrease with increasing age. Furthermore, with increasing size and, therefore, age, the number and density of secondary osteons also increase (Klein & Sander, 2008). Moreover, there would be a good correspondence between the HOS and body size (Sander, 2000; Klein & Sander, 2008; Klein *et al.*, 2009). From a correlation between the size of the femur and HOS, it has been possible to build growth curves in various taxa (Gallina, 2012). Taking the latter into account, the relationship between the estimated length of the *Kaijutitan* femur (~200 cm, see Filippi *et al.*, 2019) and its probable HOS-13 (Filippi, 2021) is consistent with the data provided by known growth curves for other sauropods (Klein & Sander, 2008, figs. 4, 5). Moreover, the neurocranium presents its preserved elements completely fused and in the case of the vertebrae examined (both the anterior cervical vertebra and the anterior caudal vertebra) none present evidence of a neurocentral suture, so that the complete fusion of the centers with its neural arches (Brochu, 1996) would also support the adult state of the specimen.

The histological observations showed the existence of "type G" bone tissue from Klein & Sander (2008, fig. 3F) characterized by a complete remodeling of the primary cortex by secondary osteons (HOS-13). This stage probably indicates that it would have reached sexual maturity at the time of death, that is, it would be somatically mature.

Bone diagenesis

The analysis of the bone microstructure of *Kaijutitan* shows poor preservation probably related to diagenetic processes occurring within the depositional environment. The small pore spaces in compact and spongy bone are usually filled with a single mineral phase of iron oxides or calcite (fibrous, drusy, or blocky) or with an iron oxide-calcite association. The calcite occurred at deeper levels in the soil and some cases show iron enrichment. This indicates local reducing conditions under the water table during precipitation, as it was described in previous research (*e.g.*, Behrensmeyer *et al.*, 1995; Retallack, 2001; Clarke, 2004; Previtera, 2017). The bones show micro-scale fractures, both in the cortex and the trabecular zone, which were cemented by sediments, iron oxides, or calcite depending on the bone, during different fossil-diagenetic stages. Radial microcracks seen in some secondary osteons are interpreted as bone desiccation cracks (Pfretzschner & Tütken, 2011). They suggest hot and semi-arid to arid climatic conditions (Pfretzschner & Tütken, 2011) that affected the bones on the surface.

Therefore, both microcracks and weathering stages observed in the *Kaijutitan* specimen indicate that its skeleton was exposed on the surface after the death of the animal for several years under warm, dry climatic conditions, at least seasonally, within the floodplain. This is consistent with the characteristics of the pelitic facies of the Sierra Barrosa Formation that would have developed in periods of water deficit, favoring the production of fine condensate-type deposits and the generation of channels with low carrying capacity (Milana, 1994; Garrido, 2011). In the distal floodplain, deposits are characterized by a low sedimentation rate with little to no degree of bone mobilization (Casal *et al.*, 2014b). There, sedimentation occurs mainly by settling of fine particles or sporadic overflow that reaches distal areas far from the channel. Here, the bones can remain weathering for much longer due to the low sedimentation rate (Casal *et al.*, 2023). However, paleoclimatic studies of the Sierra Barrosa Formation are needed to expand paleoenvironmental knowledge of the studied area. Similar diagenetic features have been identified in other vertebrate remains (*e.g.*, González Riga & Astini, 2007; González Riga *et al.*, 2009; Previtera *et al.*, 2013, 2016; Previtera, 2017, 2019a, 2019b; Mancuso & Previtera, 2022).

Finally, the *Kaijutitan* bones analyzed here come from floodplain facies of fluvial systems, in contrast to those observed in other localities of northern Patagonia such as Rincón de los Sauces (Calvo & González Riga, 2003), and southern Chubut (Casal *et al.*, 2013, 2014), in which dinosaur remains come from the overbank facies of these systems.

CONCLUDING REMARKS

The taphonomic and histological analyses of *Kaijutitan maui* determined that it corresponds to a giant adult specimen whose bones were found disarticulated but associated, largely respecting its relative anatomical position, within the floodplain.

Histological examination reveals a complete remodeling of the primary bone by secondary osteons and presence of poor vascularization (HOS-13), which, according to Klein & Sander (2008), supports the adult state of the specimen. This stage probably indicates that it would have reached sexual maturity at the time of death. The absence of growth marks and EFS is interpreted as a product of the intense remodeling of the bone matrix, as well as diagenetic processes after the burial. Biostratinomic processes include subaerial biodegradation, disarticulation, preburial weathering (cracking and flaking), exposure of spongy bone, and abrasion. Breakage surfaces show the characteristics of pre- and post-mineralization fracturing. The breakage, wear and disarticulation of the skeletal remains suggest a sub-aerial exposure and dispersion on the floodplain surface; probably due to the intervention of biological agents on the carcass scattering the bones at the quarry. Subsequently, episodes of flooding of the alluvial plain would have buried the remains of the specimen.

Fossil-diagenetic processes observed comprise: fracturing, compaction, deformation, and permineralization events. Vascular canals and fractures were cemented by iron minerals and carbonates during the burial history.

ACKNOWLEDGMENTS

We wish to thank the Municipality of Rincón de los Sauces for the logistical support provided, to the technicians of the Museo Municipal Argentino Urquiza for their active participation during the fieldwork. This work is part of one of the chapters of the Doctoral Thesis of the first author (LSF). Finally, we are particularly grateful to the comments and suggestions by the Editor J.L. Carballido, and the reviewers I. Cerda and G. Casal. The samples of *Kaijutitan* analyzed were subsidized by the PICT-2015-1021(to IC). Financial support for this work was provided by the Fund for Scientific and Technological Research, PICT-2012-I-INVI-00513 (to LSF).

REFERENCES

Alcalá, L. (1994). *Macromamíferos Neógenos de la Fosa de Alfambra-Teruel*. Instituto de Estudios Turolenses, Museo Nacional de Ciencias Naturales.

Bailleul, A. M., O'Connor, J., & Schweitzer, M. H. (2019). Dinosaur paleohistology: review, trends and new avenues of investigation. *PeerJ*, *7*, e7764. https://doi.org/10.7717/peerj.7764

Baiano, A. B. & Filippi, L. S. (2022). Allosauroid (Theropoda, Tetanurae) remains from the Sierra Barrosa Formation (Middle Coniacian, Upper Cretaceous), Patagonia, Argentina. *Publicación Electrónica de la Asociación Paleontológica Argentina*, *22*(1), 1–10.

Behrensmeyer, A. K. (1975). The taphonomy and paleoecology of Plio–Pleistoceno vertebrate assemblages east of Lake Rudolf, Kenya. *Bulletin of the Museum of Comparative Zoolology of Harvard*, *146*, 473–578.

Behrensmeyer, A. K. (1978). Taphonomic and ecologic information from bone weathering. *Paleobiology*, *4*, 150-162.

Behrensmeyer, A. K. (1991). Terrestrial vertebrate accumulations. In P. A. Allison & D. E. G. Briggs (Eds.), *Taphonomy. Releasing the data locked in the fossil record* (pp. 291–335). Plenum Press.

Botfalvai, G., Csiki-Sava, Z., Grigorescu, D., & Vasile, S. (2017). Taphonomical and palaeoecological investigation of the Late Cretaceous (Maastrichtian) *Tuştea* vertebrate assemblage (Romania; Haţeg Basin) - insights into a unique dinosaur nesting locality. *Palaeogeography, Palaeoclimatology, Palaeoecology*, *468*, 228–262.

Botha-Brink, J., Soares, M. B., & Martinelli, A. G. (2018). Osteohistology of Late Triassic prozostrodontian cynodonts from Brazil. *PeerJ*, *6*, e5029. https://doi.org/10.7717/ peerj.5029

Bridge, J. S. (2003). *Rivers and floodplains*. Blackwell Publishing.

Britt, B. B., Eberth, D. A., Scheetz, R., & Greenhalgh, B. (2004). Taphonomy of the DaltonWells dinosaur quarry (Cedar Mountain Formation, Lower Cretaceous, Utah). *Journal of Vertebrate Paleontology*, *24*(3), 41A.

Britt, B. B., Eberth, D. A., Scheetz, R. D., Greenhalgh, B. W., & Stadtman, K. L. (2009). Taphonomy of debris- flow hosted dinosaur bonebeds at Dalton Wells, Utah (Lower Cretaceous, Cedar Mountain Formation, USA). *Palaeogeography, Palaeoclimatology, Palaeoecology*, *280*, 1–22.

Brown, C. M., Evans, D. C., Campione, N. E., O'Brien, L. J., & Eberth, D. A. (2013). Evidence for taphonomic size bias in the Dinosaur Park Formation (Campanian, Alberta), a model Mesozoic terrestrial alluvial-paralic system. *Palaeogeography, Palaeoclimatology, Palaeoecology*, *372*, 108–122.

Brochu, C. A. (1996). Closure of neurocentral sutures during crocodilian ontogeny: implications for maturity assessment in fossil archosaurs. *Journal of Vertebrate Paleontology*, *16*, 49–62.

Buffetaut, E. & Suteethorn, V. (1989). A sauropod skeleton associated with theropod teeth in the Upper Jurassic of Thailand: Remarks on the taphonomic and palaeoecological significance of such associations. *Palaeogeography, Palaeoclimatology, Palaeoecology*, *73*, 77–83.

Calvo, J. O. & González Riga, B. J. (2003). *Rinconsaurus caudamirus* gen. et sp. nov., a new titanosaurid (Dinosauria, Sauropoda) from the Late Cretaceous of Patagonia, Argentina. *Revista Geológica de Chile*, *30*, 333–353.

Calvo, J. O., Porfiri, J. D., González Riga, B. J., & Kellner, A. W. A. (2007). Anatomy of *Futalognkosaurus dukei* Calvo, Porfiri, González Riga & Kellner, 2007 (Dinosauria, Titanosauridae) from the Neuquén Group (Late Cretaceous), Patagonia, Argentina. *Arquivos do Museu Nacional*, *65*, 511–526.

Canudo, J. I., Oms, O., Vila, B., Galobart, A., Fondevilla, V., Puertolas-Pascual, E., Selles, A. C., Cruzado-Caballero, P., Dinares-Turelle, J., Vicens, E., Castanera, D., Company, J., Burrel, L., Estrada, R., Marmi, J., & Blanco, A. (2016). The upper Maastrichtian dinosaur fossil record from the southern Pyrenees and its contribution to the topic of the Cretaceouse Palaeogene mass extinction event. *Cretaceous Research*, *57*, 540–551.

Casal, G. A., Martínez, R. D., Ibiricu L. M., González Riga, B., & Foix, N. (2013). Tafonomía del dinosaurio terópodo *Aniksosaurus darwini*, Formación Bajo Barreal, Cretácico Tardío de Patagonia, Argentina. *Ameghiniana*, *50*, 571–592.

Casal, G. A., Ibiricu, L. M., Allard, J. O., Martínez, R. D., Luna, M., González Riga, B., (2014a). Tafonomía del titanosaurio *Aeolosaurus colhuehuapensis,* Cretácico Superior, Patagonia central, Argentina: un ejemplo de preservación en facies continentales fluviales. *Revista Mexicana de Ciencias Geológicas*, *31*, 163–173.

Casal, G. A., Foix, N., Allard, J. O., González Riga, B. J., & Ibiricu, L. M. (2014b). Controles tafonómicos y sedimentológicos en la preservación de dinosaurios en la Fm. Bajo Barreal, Cretácico Superior, Patagonia Argentina. *Actas XIX Congreso Geológico Argentino* (pp. 777–778). Córdoba.

Casal, G. A., Ibiricu, L. M., Alvarez, B. N., Cardozo, N. V., Caglianone, J., Luna, M., & Foix, N. (2023). Procesos bioestratinómicos actuantes en *Katepensaurus goicoecheai*: Análisis de factores intrínsecos y extrínsecos. Formación Bajo Barreal (Cretácico Superior), Patagonia, Argentina. *Publicación Electrónica de la Asociación Paleontológica Argentina*, *23*(2), 1–26.

Cazau, L. B. & Uliana, M. A. (1973). El Cretácico superior continental de la Cuenca Neuquina. *Actas V° Congreso Geológico Argentino* (pp. 131–163). Córdoba.

Cerda, I. A. & Chinsamy, A. (2012). Biological implications of the bone microstructure of the Late Cretaceous Ornithopod Dinosaur *Gasparinisaura cincosaltensis*. *Journal of Vertebrate Paleontology*, *32*(2), 355–368.

Cerda, I. A., Gasparini, Z., Coria, R. A., Salgado, L., Reguero, M., Ponce, D., Gonzalez, R., Jannello, M., & Moly, J. (2019). Paleobiological inferences for the Antarctic dinosaur *Antarctopelta oliveroi* (Ornithischia: Ankylosauria) based on bone histology of the holotype. *Cretaceous Research*, *103*, 104171.

Cerda, I. A., Pereyra, M. E., Garrone, M., Ponce, D., Navarro, T. G., González, R., Militello, M., Luna, C. A., & Jannello, J. M. (2020). A basic guide for sampling and preparation of extant and fossil bones for histological studies. *Publicación Electrónica de la Asociación Paleontológica Argentina*, *20*(1), 15–28.

Chinsamy, A. (1997). Assessing the biology of fossil vertebrates through bone histology. *Palaeontologia Africana*, *33*, 29–35.

Chinsamy, A. & Dodson, P. (1995). Inside a dinosaur bone. *American Scientist*, *83*, 174-180.

Chinsamy, A. & Raath, M. A. 1992. Preparation of fossil bone for histological examination. *Palaeontologia Africana*, *29*, 39–44.

Chinsamy-Turan, A. (2005). *The Microstructure of dinosaur bone*. The Johns Hopkins University Press.

Chure, D. J., Fiorillo, A. R., & Jacobsen, A. (1998). Prey bone utilization by predatory dinosaurs in the Late Jurassic of North America, with comments on prey bone use by dinosaurs throughout the mesozoic. *Gaia*, *15*, 227-232.

Company, J. (2011). Bone histology of the titanosaur *Lirainosaurus astibiae* (Dinosauria: Sauropoda) from the Latest Cretaceous of Spain. *Naturwissenschaften*, *98*, 67–78.

Coria R. A. & Currie P. J. (2016). A New Megaraptoran Dinosaur (Dinosauria, Theropoda,

Megaraptoridae) from the Late Cretaceous of Patagonia. *PLoS ONE*, *11*(7), e0157973. https://doi.org/10.1371/journal.pone.0157973

Cormack, D. (1987). *Ham's histology*. Lippincot Company.

Curry, K. A. (1999). Ontogenetic histology of *Apatosaurus* (Dinosauria: Sauropoda): new insights on growth rates and longevity. *Journal of Vertebrate Paleontology*, *19*, 654–665.

Cruzado-Caballero, P., Gasca, J. M., Filippi, L. S, Cerda, I. A., & Garrido, A. C. (2019). A new ornithopod dinosaur from the Santonian of Northern Patagonia (Rincón de los Sauces, Argentina). *Cretaceous Research*, *98*, 211–229.

Dai, H., Xing, L., Marty, D., Zhang, J., Persons, W. S., Hu, H., & Wang, F. (2015). Microbially-induced sedimentary wrinkle structures and possible impact of microbial mats for the enhanced preservation of dinosaur tracks from the Lower Cretaceous Jiaguan Formation near Qijiang (Chongqing, China). *Cretaceous Research*, *53*, 98–109.

Digregorio, J. H. & Uliana, M. A. (1980). Cuenca Neuquina. *Academia Nacional de Ciencias de Córdoba*, *2*, 985–1032.

D'Emic, M. D. (2012). The early evolution of titanosauriform sauropod dinosaurs. *Zoological Journal of the Linnean Society*, *166*, 624–671.

Eberth, D. A. & Currie, P. J. (2010). Stratigraphy, sedimentology and taphonomy of the Albertosaurus bonebed (Upper Horseshoe Canyon Formation; Maastrichtian), southern Alberta, Canada. *Canadian Journal of Earth Sciences*, *47*, 1119–1143.

Eberth, D. A., Britt, B. B., Scheetz, R., Stadtman, K. L., & Brinkman, D. B. (2006). Dalton Wells: geology and significance of debris-flow-hosted dinosaur bonebeds in the Cedar Mountain Formation (Lower Cretaceous) of eastern Utah, USA. *Palaeogeography, Palaeoclimatology, Palaeoecology*, *236*, 217–245.

Enlow, D. H. & Brown, S. O. (1957). A comparative histological study of fossil and recent bone tissue. Pt. 1. *Texas Journal of Science*, *8*, 405–443.

Erickson, G. M. & Tumanova, T. A. (2000). Growth curve of *Psittacosaurus mongoliensis* Osborn (Ceratopsia: Psittacosauridae) inferred from long bone histology. *Zoological Journal of the Linnean Society*, *130*, 551–566.

Erickson, G. M., Makovicky, P. J., Currie, P. J., Norell, M. A., Yerby, S. A., & Brochu, C. A. (2004). Gigantism and comparative life-history parameters of tyrannosaurid dinosaurs. *Nature*, *430*, 772–775.

Fernández López, S. (1989). La materia fósil. Una concepción dinamicista de los fósiles. In E. Aguirre (Ed.) *Paleontología Nuevas Tendencias*, (pp. 25–45).

Fernández López, S. (2000). *Temas de Tafonomía*. Departamento de Paleontología, Universidad Complutense de Madrid.

Filippi, L. S. (2021). *Los dinosaurios saurópodos de la Formación Sierra Barrosa (Coniaciano), Grupo Neuquén, en el área de Rincón de los Sauces (Neuquén): osteología, relaciones filogenéticas e inferencias paleobiogeográficas* [Unpublished PhD Thesis]. Universidad Nacional del Comahue, Centro Regional Universitario Bariloche.

Filippi, L. S., Salgado, L., & Garrido, A. C. (2019). A new giant basal titanosaur sauropod in the Upper Cretaceous (Coniacian) of the Neuquén Basin, Argentina. *Cretaceous Research*, *100*, 61–81.

Francillon-Vieillot, H., De Buffrénil, V., Castanet, J., Geraudie, J., Meunier, F. J., Sire, J. Y., Zylberberg, L., & De Ricqlès, A. (1990). Microstructure and mineralization of vertebrate skeletal tissues. In J. G. Carter (Ed.) *Skeletal Biomineralization: Patterns, Processes and Evolutionary Trends* (pp. 471–530). Van Nestrand Reinhold.

Franzese, J., Spalletti, L., Gómez Pérez, I., & Macdonald, D. (2003). Tectonic and paleoenviromental evolution of Mesozoic sedimentary basins along the Andean foothills of Argentina (32°-54°S). *Journal of South American Earth Sciences*, *16*, 81–90.

Gallina, P. A. (2012). Histología ósea del Titanosaurio *Bonitasaura salgadoi* (Dinosauria: Sauropoda) del Cretácico Superior de Patagonia. *Ameghiniana*, *49*(3), 289–302.

Garrido, A. C. (2010). Estratigrafía del Grupo Neuquén, cretácico Superior de la Cuenca Neuquina (Argentina): nueva propuesta de ordenamiento litoestratigráfico. *Revista del Museo Argentino de Ciencias Naturale*s, *12*, 121–177.

Garrido, A. C. (2011). El Grupo Neuquén (Cretácico Tardío) en la Cuenca Neuquina. In G*eología y Recursos Naturales de la Provincia del Neuquén, 18º Congreso Geológico Argentino*, *21* (pp. 231–244). Neuquén.

González Riga, B. J. (2003). A new titanosaur (Dinosauria, Sauropoda) from the Upper Cretaceous of Mendoza Province, Argentina. *Ameghiniana*, *40*(2), 155–172.

González Riga, B. J. & Astini, R. A. (2007). Preservation of large titanosaur sauropods in overbank fluvial facies: A case study in the Cretaceous of Argentina. *Journal of South American Earth Sciences*, *23*, 290–303

González Riga, B. J., Previtera, E., & Pirrone, C. A. (2009). Malarguesaurus florenciae gen. et sp. nov., a new titanosauriform (Dinosauria, Sauropoda) from the Upper Cretaceous of Mendoza, Argentina. *Cretaceous Research*, *30*, 135–148.

González Riga, B. J., Lamanna, M. C., Ortiz David, L., Calvo, J. O., & Coria, J. P. (2016). A gigantic new dinosaur from Argentina and the evolution of the sauropod hind foot. *Scientific Reports*, *6*, 19165.

Grigorescu, D. & Csiki, Z. (2002). Conference Field Trip - Geological introduction to the uppermost Cretaceous continental formations with dinosaurs and other vertebrates of the Haţeg Basin. In D. Grigorescu & Z. Csiki (Eds.) *7th European Workshop on Vertebrate Palaeontology* (pp. 50–69). Sibiu, Rumania.

Haynes, G. (1980). Evidence of carnivore gnawing on Pleistocene and Recent mammalian bones. *Paleobiology*, *6*, 341–351.

Hedrick, B. P., Tumarkin-Deratzian, A. R., & Dodson, P. (2014). Bone microstructure and relative age of the holotype specimen of the diplodocoid sauropod dinosaur *Suuwassea emilieae. Acta Palaeontologica Polonica*, *59*(2), 295–304.

Herrero Ducloux, A. (1938). *Reconocimiento de la zona situada entre la vía férrea, el río Neuquén y el meridiano de Plaza Huincul*. Yacimientos Petrolíferos Fiscales.

Horner, J. R., Ricqlès, A. J., & Padian, K. (2000). Long bone histology of the hadrosaurid dinosaur *Maisaura peeblesorum*: growth dynamics and physiology based on an ontogenetic series of skeletal elements. *Journal of Vertebrate Paleontology*, *20*, 115–129.

Howell, J. A., Schwarz, E., Spalletti, L. A., & Veiga, G. D. (2005). The Neuquén Basin: an overview. In G. D. Veiga, L. A. Spalletti, J. A. Howell, & E. Schwarz (Eds.) *The Neuquén Basin, Argentina: A Case Study in Sequence Stratigraphy and Basin Dynamics* (pp. 1–14). Geological Society Special Publications.

Ibiricu, L. M., Martínez, R. D., Casal, G. A., & Cerda, I. A. (2013). The Behavioral Implications of a Multi-Individual Bonebed of a Small Theropod Dinosaur. *PloS ONE*, *8*(5), e64253. https://doi.org/10.1371/journal.pone.0064253

Jordana, X., Marín-Moratalla, N., Moncunill-Solèa, B., Nacarino-Meneses, C., & Köhler, M. (2016). Ontogenetic changes in the histological features of zonal bone tissue of ruminants: A quantitative approach. *Comptes Rendus Palevol*, *15*, 255–266.

Kidwell, S. M., Fürsich, F. T., & Aigner, T. (1986). Conceptual framework for the analysis and classification of fossil concentrations. *Palaios*, *1*(3), 228–238.

Klein, N. & Sander, P. M. (2008). Ontogenetic stages in the long bone histology of sauropod dinosaurs. *Paleobiology*, *34*, 247–263.

Klein, N., Sander, P. M., & Suteethorn, V. (2009). Bone histology and its implications for the life history and growth of the Early Cretaceous titanosaur *Phuwiangosaurus sirindhornae*. *Geological Society Special Publications*, *315*, 217–228.

Leanza, H. A. & Hugo, C. A. (2001). Hoja Geológica 3969-I-Zapala, provincia del Neuquén. Instituto de Geología y Recursos Naturales. *Boletín Servicio Geológico Nacional*, *275*, 1–128.

Leanza, H. A., Apesteguía, S., Novas, F. E., & De la Fuente, M. S. (2004). Cretaceous terrestrial beds from the Neuquén basin (Argentina) and their tetrapod assemblages. *Cretaceous Research*, *25*, 1–96.

Legarreta, L. & Gulisano, C. A. (1989). Análisis estratigráfico secuencial de la Cuenca Neuquina (Triásico superior–Terciario inferior). In G. Chebli & L. Spalletti (Eds.), *Cuencas Sedimentarias Argentinas. X° Congreso Geológico Argentino. Serie Correlación Geológica*, *6*, 221–243.

Legarreta, L. & Uliana, M. A. (1991). Jurassic-Cretaceous marine oscillations and geometry of back-arc basin fill, central Argentine Andes. In D. I. MacDonald (Ed.) *Sedimentation, Tectonics and Eustasy: Sea level Changes at Active Plate Margin* (pp. 429–450). International Association of Sedimentologists Special Publication 12.

Lyman, R. L. (1994). *Vertebrate taphonomy*. Cambridge University Press.

Mancuso, A. C. & Previtera, E. (2022). Bone diagenesis of tetrapods from the Middle Triassic Tarjados Formation: implication for depositional environment and palaeoclimate. *Palaeobiodiversity and Palaeoenvironments*, *102*, 205–221. https://doi.org/10.1007/s12549-021-00500-4

Milana, J. P. (1994). Secuencias aluviales asociadas a variaciones hidrológicas: consideraciones teóricas y ejemplos. *Revista de la Asociación Argentina de Sedimentología*, *1*(2), 103–124.

Mitchell, J. & Sander, P. M. (2014). The three-front model: a developmental explanation of long bone diaphyseal histology of Sauropoda. *Biological Journal of the Linnean Society*, *112*(4), 765–781. https://doi.org/10.1111/bij.12324

Mitchell, J., Sander, P. M, & Stein, K. (2017). Can secondary osteons be used as ontogenetic indicators in sauropods? Extending the histological ontogenetic stages into senescence. *Paleobiology*, *43*(2), 321–342.

Padian, K. & Lamm, E. T. (2013). *Bone Histology of Fossil Tetrapods: Advancing Methods, Analysis, and Interpretation*. University of California Press.

Paik, I. S., Kim, H. J., Park, K. H., Song, Y. S., Lee, Y. I., Hwang, J. Y., & Huh, M. (2001). Paleoenvironments and taphonomic preservation of dinosaur bone-bearing deposits in the Lower Cretaceous Hasandong Formation, Korea. *Cretaceous Research*, *22*, 627–642.

Pfretzschner, H. U. & Tütken, T. (2011). Rolling bones – taphonomy of Jurassic dinosaur bones inferred from diagenetic microcraks and mineral infillings. *Palaeogeography, Palaeoclimatology, Palaeoecology*, *310*, 17–123.

Previtera, E. (2013). Tafonomía de vertebrados del Cretácico Superior de la Formación Loncoche en Calmuco (Mendoza, Argentina): implicancias paleoambientales y paleogeográficas. *Ameghiniana*, *50*, 483–492.

Previtera, E. (2017). Bone microstructure and diagenesis of saurischian dinosaurs from the Upper Cretaceous (Neuquén Group), Argentina. *Andean Geology*, *44*, 39–58.

Previtera, E. (2019a). Taphonomic analysis of saurischian dinosaurs from the Plottier Formation (Upper Cretaceous), Mendoza, Argentina. *Andean Geology*, *46*(2), 345–367.

Previtera, E. (2019b). Diagenetic characterization of dinosaur remains trough histology in fluvial contexts from the Upper Cretaceous of Loncoche Formation, Mendoza, Argentina. *Ameghiniana*, *56*(2), 135–152.

Previtera, E., D'angelo, J. A., & Mancuso, A. C. (2013). Preliminary chemometric study of bone diagenesis in Early Triassic cynodonts from Mendoza, Argentina. *Ameghiniana*, *50*, 460–468.

Previtera, E., Mancuso, A. C., De La Fuente, M. S., & Sánchez, E. S. (2016). Diagenetic analysis of tetrapod from the Upper Triassic, Puesto Viejo Group, Argentina. *Andean Geology*, *43*(2), 197–214.

Ramos, V. A. (1981). Descripción Geológica de la Hoja 33c, Los Chihuidos Norte. Provincia del Neuquén. *Boletín Servicio Geológico Nacional*, *182*, 1–103.

Reid, R. E. H. (1996). Bone histology of the Cleveland-Lloyd dinosaurs and of dinosaurs in general. Part I: introduction to bone tissues. *Brigham Young University Geology Studies*, *41*, 25–72.

Sander, P. M. (2000). Longbone histology of the Tendaguru sauropods: implications for growth and biology. *Paleobiology*, *26*, 466–488.

Schwarz, E. (2012). Sharp-based marine sandstone bodies in the Mulichinco Formation (Lower Cretaceous), Neuquén Basin, Argentina: remnants of trans gressive offshore sand ridges. *Sedimentology*, *59*, 1478–1508.

Shipman, P. (1981). *Life History of a fossils*. Harvard University Press.

Tomassini, R. L., Montalvo, C. I., Manera, T., & Oliva, C. (2010). Estudio tafonómico de los mamíferos pleistocenos del yacimiento de Playa del Barco (Pehuen Co), provincia de Buenos Aires, Argentina. *Ameghiniana*, *47*, 137–152.

Smith, R. M. H., Sidor, C. A., Tabor, N. J., & Steyer, J. S. (2015). Sedimentology and vertebrate taphonomy of the Moradi Formation of northern Niger: A Permian wet desert in the tropics of Pangaea. *Palaeogeography, Palaeoclimatology, Palaeoecology*, *440*, 128–141.

Stein, K., Csiki, Z., Curry Rogers, K. A., Weishampel, D. B., Redelstorff, R., Carballido, J. L., & Sander, P. M. (2010). Small body size and extreme cortical bone remodeling indicate phyletic dwarfism in *Magyarosaurus dacus* (Sauropoda: Titanosauria). *Proceeding of the Natural Academy of Sciences*, *107*, 9258–9263.

Steyer, J. S., Laurin, M., Castanet, J., & de Ricqlès, A. J. (2004). First histological and skeletochronological data on temnospondyl growth; palaeoecological and palaeoclimatological implications. *Palaeogeography, Palaeoclimatology, Palaeoecology*, *206*, 193–201.

Voorhies, M. R. (1969). Taphonomy and population dynamics of the early Pliocene vertebrate fauna, Knox County, Nebraska. *Contributions of the Geological Society, Special Papers*, *1*, 1–69.

Wings, O., Sander, P. M., Tutken, T., Fowler, D., & Sun, G. (2007). Growth and life history of Asia's largest dinosaur. *Journal of Vertebrate Paleontology*, *27*, 167A.

Woodward, H. N. (2019). *Maiasaura* (Dinosauria: Hadrosauridae) tibia osteohistology reveals non-annual cortical vascular rings in young of the year. *Frontiers in Earth Sciences*, *7*, 50. https://doi.org/10.3389/feart.2019.00050

Woodward, H. N. & Lehman, T. M. (2009). Bone histology of and microanatomy of *Alamosaurus sanjuanensis* (Sauropoda: Titanosauria) from the Maastrichtian of Big Bend National Park, Texas. *Journal of Vertebrate Paleontology*, *29*, 807–821.

doi: 10.5710/PEAPA/26.02.2024.481

Recibido: 18 de julio 2023

Aceptado: 26 de febrero 2024

Publicado: 17 de abril 2024